J Mater Sci (2011) 46:7501–7510
DOI 10.1007/s10853-011-5721-3

Evaluation of electrospun nanofiber formation of perfluorosulfonic acid and poly (*N*-vinylpyrrolidone) through solution rheology

Junhong Zhao · Anhou Xu · Wang Zhang Yuan · Jianbing Gao · Junke Tang · Li Wang · Fei Ai · Yongming Zhang

Received: 7 March 2011 / Accepted: 14 June 2011 / Published online: 23 June 2011

Abstract Electrospinning performance of 5–52 wt% perfluorosulfonic acid (PFSA), poly (*N*-vinylpyrrolidone) (PVP), and PFSA/PVP blends in *N*,*N*-dimethylformamide (DMF) with various PFSA/PVP ratios were systematically investigated in respective of solutions properties, mainly surface tension and rheological properties. Mechanical relaxation time τ_M calculated from rheological results happens to be closely correlated with nanofiber morphology, and is used to evaluate the electrospinnability. Polymer solutions with higher τ_M show better electrospinnability. Morphologies of the electrospun samples were observed by Scanning electronic microscopy. The results show that the pure PFSA solutions, even with a quite high concentration up to 52 wt%, fail to be electrospun and possess a very low τ_M. Addition of PVP improves electrospinnability of PFSA and increases τ_M. The electrospinnability of PFSA/PVP/DMF solutions can be manipulated by changing the ratio of PFSA to PVP and the total polymer concentration of the mixed solutions. The PFSA nanofiber mats with a small fraction of PVP (<8 wt%) with the average diameter of 370 nm were successfully obtained.

J. Zhao · A. Xu · W. Z. Yuan · F. Ai · Y. Zhang (✉)
School of Chemistry and Chemical Engineering, Shanghai Jiao Tong University, No. 800 Dongchuan Rd, Shanghai 200240, People's Republic of China
e-mail: ymzsjtu@yahoo.com.cn

J. Gao
College of Chemical and Food Engineering, Zhongzhou University, No. 6 Yingcai Rd, Zhengzhou 450044, People's Republic of China

J. Tang · L. Wang
Shandong Dongyue Polymer Material Co. Ltd., Zibo 256400, People's Republic of China

Introduction

Electrospinning has been widely used to construct a variety of non-woven membranes with interconnected nanofiber structure and a much higher surface area per volume [1–4]. The special properties arising from their physical structure, functional chemical composition, and kinetic processing approach allow the electrospun nanofiber membranes to achieve a broad range of applications such as scaffolds for tissue engineering [5, 6], drug delivery devices [7], fields of filtration and separation [8, 9], multifunctional membranes [10, 11], nanocomposites [12], and sensors [13].

Perfluorosulfonic acid which consists of a perfluorinated backbone and perfluorovinyl ether pendant chains terminated by sulfonic head groups (Scheme 1), possess many interesting properties with respect to super selectivity and facile cation transport, high mechanical strength, good thermal stability, and chemical-biological inertness. Therefore, PFSA has found various applications in fuel cells [14], chlor-alkali production [15], metal ion recovery [16], gas drying or humidification [17, 18], batteries [19], sensors [20], drug release [21], and polymeric catalysts [22, 23]. Recently, fabricating PFSA membrane with interconnected nanostructure has attracted worldwide interests. Optimization of its efficacy for the demands of numerous practical applications is quite promising, such as sensors, metal ion recovery, and catalyst layers of proton exchange membrane fuel cells [24–26]. However, successful electrospun pure PFSA nanofiber has not been reported.

Despite the simplicity of the electrospinning setup, the actual mechanism of nanofiber formation is rather complex. The electrospinning process is affected by various solution properties such as polymer conformations in solution, rheological properties, electrical conductivity, and surface tension [27, 28]. In addition, operating conditions

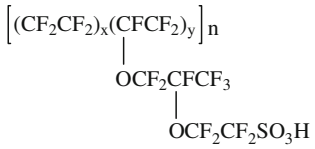

Scheme 1 Structure of PFSA

such as the applied voltage, the tip-to-collector distance, and the feed rate of the polymer solution also influence the electrospinning process. Electrospinning of polyelectrolytes has been considered to be a challenging work due to the existence of static electric interactions [26]. In many cases, researchers have to use mixed solvents, additive polymers or by additional treatment to make solutions compatible to the electrospinning process [29–31]. Hence, it is important to investigate related changes in solutions properties of PFSA varying in compositions or treatment to find the optimized conditions for electrospinning. There have been several studies on relatively dilute solutions of PFSA [32, 33]. However, little is known about the solution properties of PFSA, especially rheological properties, which is closely related to electrospinnability. Electrospinning of Nafion (1100EW) in DMF over a concentration range of 25–35 wt% have been evaluated in Chen's study [26] and their electrospinning experiments have not referred to the Nafion solutions in DMF at an even higher concentration.

In this study, the PFSA from Shandong Dongyue Shenzhou New Material Co. Ltd, China (932 EW, corresponding ion exchange capacity is 1.18 mmol/g) in DMF were electrospun. Effects of poly (*N*-vinylpyrrolidone) (PVP) ($M_W = 1300{,}000$) on the solution properties and fiber performance of PFSA solutions were systematically characterized by rheological behavior, surface tension, and SEM. The electrospinning diagram of a PFSA/PVP/DMF ternary system was established for preparing PFSA/PVP nanofiber membranes with porous and interconnected structure, which could find potential applications in sensors, metal ion removal, drug release, proton exchange membranes, and catalytic layer of fuel cells.

Experiments

Materials and sample preparations

Poly (*N*-vinylpyrrolidone) ($M_W = 1300{,}000$) was purchased from Alfa and utilized without any further treatments. *N*,*N*-dimethylformamide (DMF, 99%) was obtained from Sinopharm Chemical Reagent Co., Ltd. (China) and used as received. PFSA ionomer (EW 923, corresponding ion exchange capacity is 1.18 mmol/g) was provided as pellets by Dongyue Shenzhou New Materials Company Ltd., China. The PFSA pellets were cleaned in a 5 wt% hydrogen peroxide solution at 60 °C for 30 min, and further in a 1 M sulfuric acid solution at 80 °C for 30 min, then boiled in deionized water for several times. The cleaned PFSA pellets were dissolved in an ethanol/water (50/50) mixture, using an autoclave at 230 °C for 4 h. This solution was filtered with Millipore membrane and transferred into Petri dish, then dried at 40 °C. The resulting PFSA film was taken off by a scalpel and triturated into powders in a mortar. PFSA powder was dried in a vacuum oven at 80 °C for 3 h before use. The PFSA and PVP solutions were prepared by dissolving PFSA and PVP powder in DMF solvent, then agitated vigorously for 24 h. Five PFSA/PVP/DMF solutions were prepared by mixing 52 wt% PFSA/DMF solution with 12 wt% PVP/DMF solution with different ratios. The compositions of the PFSA/PVP/DMF solutions are shown in Table 1. $S_{X,Y\text{wt\%}}$ represents polymer type *X* (PFSA or PVP) with concentration of *Y* wt%. The symbol of S*x*F*y*V*z* in Table 1 and the following context represents the PFSA/PVP blend solution with the total concentration of *x* wt%, in which PFSA and PVP ratio in the blend polymers are *y* and *z* wt%, respectively.

Electrospinning

The electrospinning apparatus is composed of a BGG-type high voltage DC generator (Beijing Machinery and Electricity Institute Co., Ltd.), a KDS-220 Multi-Syringe Infusion Pump (KD Scientific Inc), a blunt-spray-nozzle connected to the syringe with a Teflon feed line, a grounded collector and other fittings. The grounded collector can be either a flat plate or a stainless steel drum.

Electrospinning of pure PFSA and pure PVP solutions were executed before the electrospinning of PFSA/PVP blend solutions. The uniform fibers can be successfully obtained from the 12 wt% PVP solution and the best spinning conditions were identified as a voltage of 8–10 kv, a tip-collector distance of 15 cm, and a relative humidity of 30–40% and 0.1–0.3 mL h^{-1} flow rate with a 0.7 mm nozzle. All electrospinning experiments of PFSA/PVP blend solutions were conducted under such conditions.

Surface tension measurements

Surface tensions were measured using the Wilhelmy method with a 4-cm periphery platinum plate on the automatic BZY-1 Model surface tension apparatus (Hengping Apparatus Co. Ltd., Shanghai, China) at room temperature.

Table 1 Compositions of five PFSA/PVP/DMF solutions

Solution symbols	$S_{PFSA,52wt\%}/S_{PVP,12wt\%}$ w/w	Total polymer concentration (PFSA, PVP)/wt%	Mass ratio of PFSA/PVP
S52F100V0	100/0	52(52,0)	100/0
S50F98.8V1.2	95/5	50(49.4,0.6)	98.8/1.2
S48F97.5V2.5	90/10	48(46.8,1.2)	97.5/2.5
S32F81.3V18.7	50/50	32(26,6)	81.3/18.7
S20F53.0V47.0	20/80	20(10.6, 9.4)	53.0/47.0
S16F32.5V67.5	10/90	16(5.2, 10.8)	32.5/67.5
S12F0V100	0/100	12(0,12)	0/100

The symbol of S*x*F*y*V*z* represents the PFSA/PVP blend solution with the total concentration of *x* wt%, in which PFSA and PVP in the blend polymers are *y* and *z* wt%, respectively

Scanning electronic microscopy

Morphology observation was carried out on a JSM-7401F (JEOL Ltd, Japan) SEM at low vacuum. Samples were spun onto aluminum foils and sputter-coated with a thin layer of gold using an Emitech K550 sputter coater with a current of 20 mA for 40 s before the SEM experiment.

Rheological measurement

Oscillatory and steady shear rheological measurements were performed using AR-G2 rheometer (TA instruments, USA) with a 60 mm diameter, 2° cone and plate geometry and a solvent trap. The steady measurements of pure PVP and PFSA/PVP mixed solutions were conducted from 0.1 to 1000 s^{-1} at 25 °C. Frequency sweeps were conducted from 100 to 0.1 rad s^{-1} under a controlled stress of 1.0 Pa within the linear region at 25 °C. The specific viscosity (η_{sp}) was calculated as follows: $\eta_{sp} = (\eta_0 - \eta_s)/\eta_s$, where η_s is the solvent viscosity and η_0 is the zero-shear viscosity. Viscosity of DMF is calculated as 0.802 mPa s at 25 °C [34]. The polymer solutions were placed in a water bath at 40 °C overnight to remove entrained air before rheological measurements.

Results and discussions

Electrospinnability of PVP solutions increased with the increase of polymer concentration (Fig. 1a–c). However, electrospinning of pure PFSA solutions in DMF at a broad concentration range of 5–52 wt% produced only droplets on the aluminum foil collector in spite of the increasing of concentration (Fig. 1d–f). As we know, the electrospinning process is complicated and whether or not the ejected stream can form nanofibers is mainly determined by the solution properties, especially the surface tension and the state of chain entanglements.

Surface tensions

It has been proposed that a lower surface tension will facilitate the fiber formation of the polymer solution. The poor electrospinnability of polyelectrolyte has been attributed to the high surface tension of the solution, which is usually close to that of the solvent [35, 36]. In our study, we use a high polar solvent, DMF, which possesses a lower surface tension than that of water.

Figure 1 shows surface tensions of PFSA/DMF and PVP/DMF solutions with concentrations of 5–52 wt% at room temperature. The surface tensions of PFSA/DMF solutions are lower than those of pure DMF and 12 wt% PVP/DMF solution. Though PFSA/DMF solutions failed to be electrospun, their surface tension values are located at 22–32 mN/m, which are normally suitable for electrospinning fine nanofiber. Therefore, surface tension could not be a barrier factor for pure PFSA solutions to form electrospun fibers.

Rheological results

Chain entanglements of polymer solutions are closely correlated with molecular weight, molecular structure, and conformations in the solvent. For a given polymer solution, one way to increase the chain entanglement density in it is to increase the polymer concentration, thus increasing its apparent viscosity. From the plot of specific viscosity (η_{sp}) versus concentration, the entanglement concentration (C_e) can be calculated at the transition between unentangled and entangled regions. In general, for electrospinning, beaded fibers begin to form at entanglement concentration C_e and bead-free fibers start to form at 2–2.5C_e [37], which is defined as "C_e-regulation" hereinafter for simplicity. As shown in Fig. 2, C_e of PVP/DMF solution is calculated at about 5.5 wt%, where the scaling relationship shifts from η_{sp}–$C^{1.03}$ to η_{sp}–$C^{4.03}$. The PVP/DMF solution begins to form beaded fibers at ~5.0 wt%, and bead-free fibers at ~12 wt% (~2.18C_e), following the "C_e-regulation" well.

Zero-shear viscosity η_0 of pure PFSA solutions are as low as 0.01 Pa s at 30 wt% (Figures not given). The pure PFSA solution with concentration of 52 wt% has a relative high η_0 of 1.0 Pa s. In addition, the scaling relationship of η_{sp} with concentration C shifts from η_{sp}–$C^{1.54}$ to η_{sp}–$C^{5.64}$ as shown in Fig. 2. The corresponding C_e of PFSA/DMF is about 27.6 wt%, at which PFSA/DMF solution does not form beaded nanofibers. The PFSA/DMF solution at 52 wt% (~2C_e) does not form uniform fiber, either. It suggests that beaded fibers begin to form at concentration

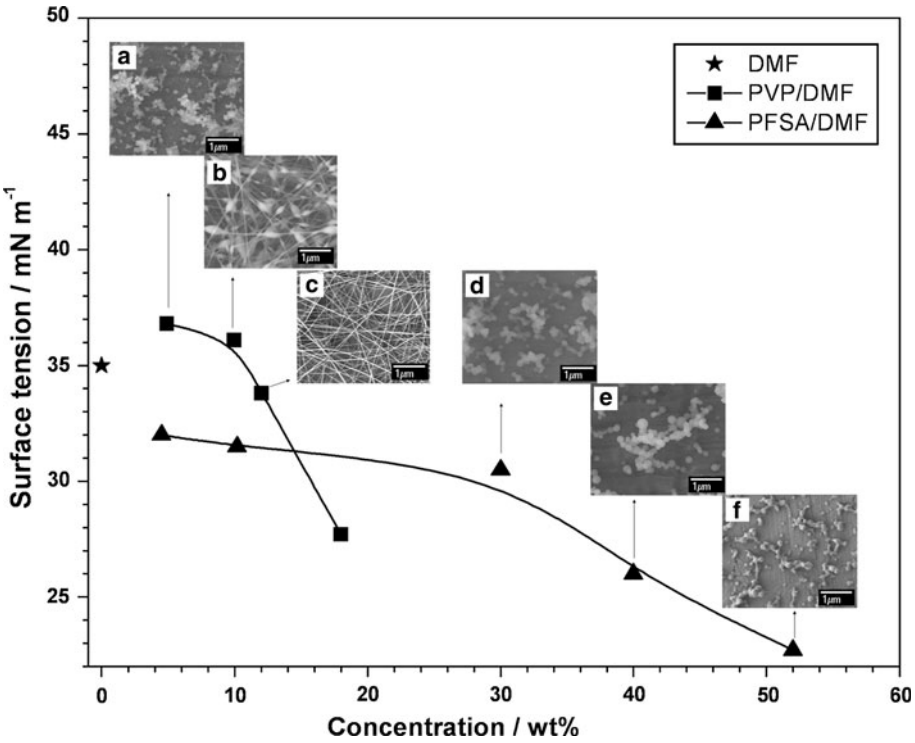

Fig. 1 Surface tensions of PFSA/DMF and PVP/DMF solutions with various concentrations at room temperature, and SEM images of electrospun PFSA/DMF and PVP/DMF solutions at corresponding concentrations of **a** 5 wt% PVP, **b** 10 wt% PVP, **c** 12 wt% PVP, **d** 30 wt% PFSA, **e** 40 wt% PFSA, and **f** 52 wt% PFSA

higher than $2C_e$. Uniform fiber formation of pure PFSA/DMF solution might require an even higher concentration than 52 wt%, which disagrees with the "C_e-regulation". However, it is impossible to prepare a PFSA solution with a much higher concentration than 52 wt% due to its poor solubility. Similar observations have been found in other polyelectrolyte electrospinning systems. Poly[2-(dimethylamino)ethyl methacrylate hydrochloride] in 80/20 (wt/wt) water/methanol could not be electrospun below $8C_e$ [38] and sulfonated polystyrene fibers were electrospun at concentration up to $3.5C_e$ [39].

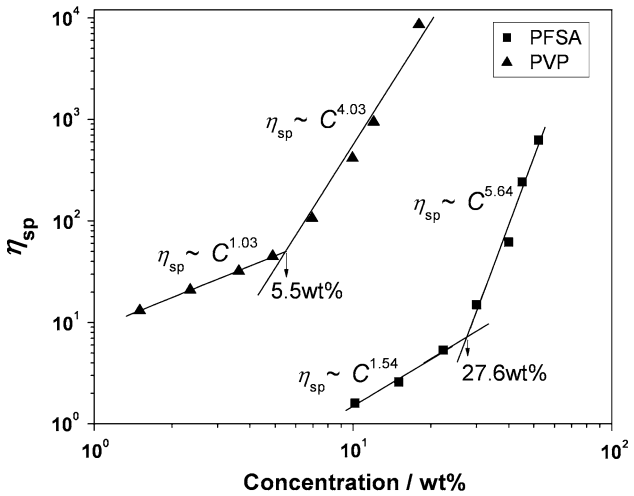

Fig. 2 Concentration dependence of specific viscosity η_{sp} for PFSA/DMF and PVP/DMF solutions at room temperature

Figure 3 shows the dynamic frequency sweeps of both PFSA/DMF and PVP/DMF solutions at 25 °C. At low frequency region, storage modulus G' and loss modulus G'' of PVP/DMF solutions is proportional to ω^2 and ω, respectively, which is a typical behavior in linear viscoelastic region as formulated by $G' = J_e\eta_0^2\omega^2$ and $G'' = \eta_0\omega$ (J_e, the steady-state compliance) [40]. The values of G' and G'' increase with the increase of polymer concentrations for both PFSA/DMF and PVP/DMF solutions. Based on Takahashi's theory, mechanical relaxation time τ_M of polymer chains in solution could be calculated as $\tau_M = J_e\eta_0$ [41]. τ_M of PFSA/DMF and PVP/DMF solutions are presented in Fig. 4. τ_M values of PFSA solutions are much lower than those of PVP solutions. It is proposed that τ_M could be a more sensitive indicator of chain entanglement for PFSA solution than zero-shear viscosity. Due to the insolubility of fluorocarbon backbone of PFSA in common polar solvent, PFSA chains may collapse into increasingly compact coils, further into aggregations with ionic side chains around their surfaces as concentration increases [42–45]. Polymer–polymer contacts in the PFSA/DMF solutions take place at the surface of the aggregation through the associating interactions between sulfonated acid ion groups and solvent, leading to relatively little inter-penetration and segment mixing between PFSA chains and thus lower τ_M values. Quite low G' or high loss factor tan δ (Figures not given) at low frequency regions suggests the poor elasticity of PFSA/DMF solutions, making PFSA/DMF difficult to be electrospun. Time-concentration superpositions (TCS) of G' and G'' of both

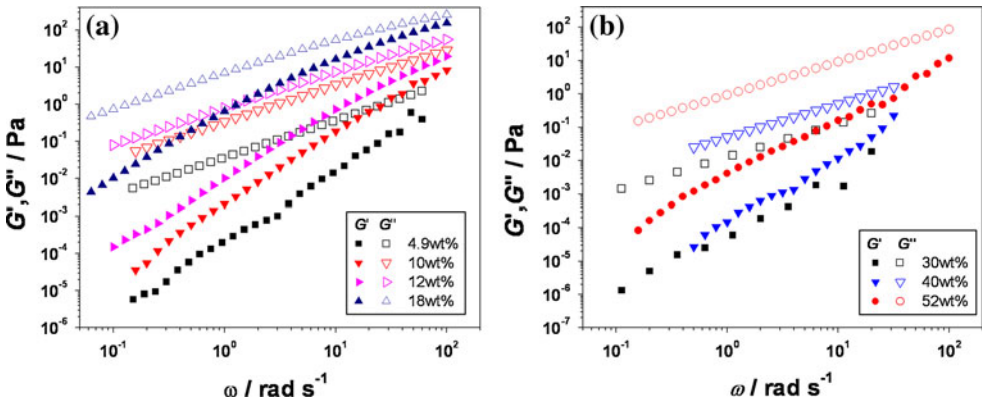

Fig. 3 Dynamic frequency sweeps of **a** PVP/DMF and **b** PFSA/DMF solutions with a controlled stress of 1.0 Pa at 25 °C

PVP/DMF and PFSA/DMF solutions were tried to get master curves for reference concentrations of 10 wt% for PVP/DMF solutions and 40 wt% for PFSA/DMF solutions, respectively, as shown in Fig. 5. Frequency shift factor a_C can be determined according to Eqs. 1 and 2:

$$G'(\omega, C_{\text{ref}}) = G'(\omega a_C, C) \quad (1)$$

$$G''(\omega, C_{\text{ref}}) = G''(\omega a_C, C) \quad (2)$$

TCS works well for PVP/DMF solutions with concentrations higher than 10 wt%, but fails at 4.9 wt%, which agrees well with the results in Fig. 2. The shift factor a_C are calculated to be 0.1, 2.5, and 20 for PVP/DMF solutions with concentrations of 4.9, 12, and 18 wt%, respectively. G' is proportional to ω at high frequencies, suggesting that the simple Rouse or Zimm models for flexible molecules is not suitable for PVP in DMF. PVP probably behaves as semi-flexible and elongated in DMF, which would facilitate electrospinning. As G' for PFSA/DMF systems, TCS fails at all three concentrations higher than C_e, which may be caused by the existence of static electronic interactions.

An effective way to enhance electrospinnability of PFSA/DMF solution is through addition of a high molecular weight polymer that can form a stable solution with PFSA and serve as a carrier. PVP, an amphiphilic polymer with a high molecular weight, is usually used as associative polymer for electrospinning. Moreover, it has been used to improve the methanol crossover property of the ion-exchange membrane, where some weak acid–base interaction can be formed between PFSA and PVP [46, 47].

Figure 6 shows the apparent viscosity η versus shear rate $\dot{\gamma}$ of the PFSA/PVP/DMF solutions at 25 °C. All solutions show first Newtonian regions followed by shear thinning regions at high shear rates. The appearance of shear thinning suggests that chain entanglements exist in PFSA/PVP/DMF solutions. Addition of PVP would shorten the first Newtonian region to low shear rates.

Figure 7 shows dynamic frequency sweeps of the PFSA/PVP/DMF solutions at 25 °C. All curves show similar shapes to that of pure PVP solutions with G'–ω^2 and G''–ω at low frequency region. τ_M of the five PFSA/PVP/DMF

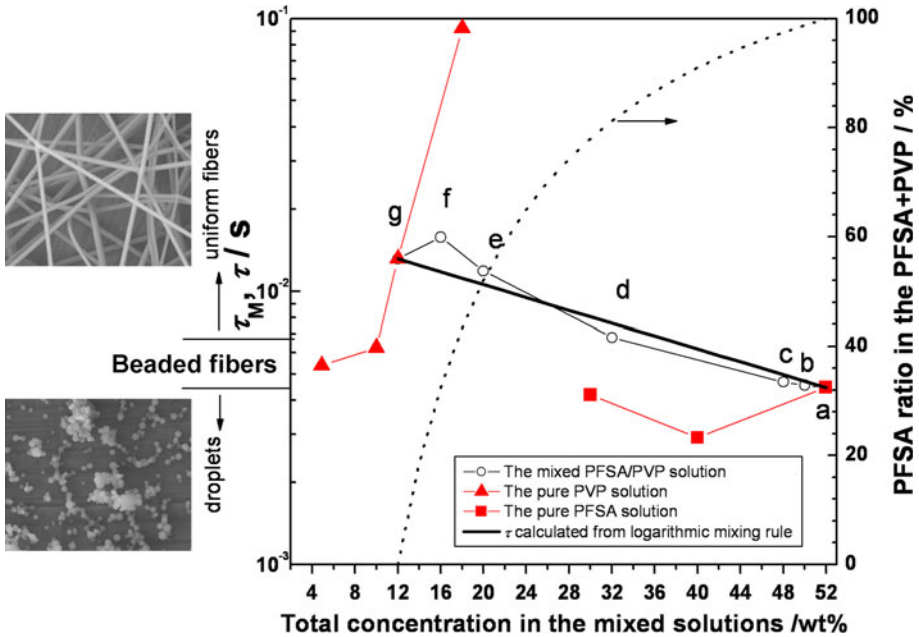

Fig. 4 Composition dependence of mechanical relaxation time τ_M of PVP/DMF, PFSA/DMF, and PFSA/PVP/DMF solutions at 25 °C. The *black solid line* presents the theoretical τ calculated from Eq. 3. The *dot line* refers to PFSA/PVP ratios of (*a*) S52F100V0, (*b*) S50F99V1.0, (*c*) S48F97.5V2.5, (*d*) S32F81.3V18.7, (*e*) S20F53.0V47.0, and (*f*) S16F32.5V67.5

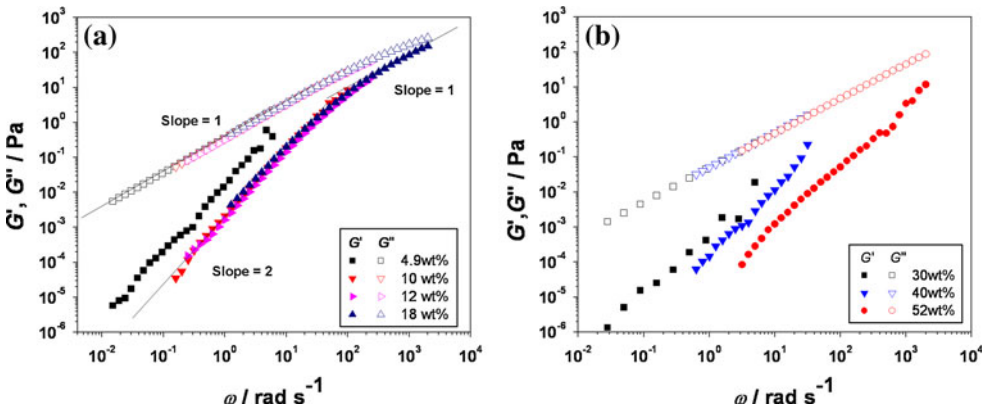

Fig. 5 G' and G'' time-concentration superpositions of **a** PVP/DMF and **b** PFSA/DMF solutions with a controlled stress of 1.0 Pa at 25 °C

solutions are presented in Fig. 4. The morphologies of the electrospun samples from these mixed solution changes from droplets, beaded fibers to uniform fibers, as shown in Fig. 8. Addition of PVP effectively enhances the electrospinnability of PFSA solutions. All observations suggest that there are specific relaxation time windows for the PFSA/PVP/DMF solutions to successfully form electrospinning fibers.

The theoretical values (τ) of the PFSA/PVP blend solutions calculated by the logarithmic mixing rule from their starting pure solutions as Eq. 3 [48, 49] are also presented in Fig. 4.

$$\log \tau(S_c F_w V_{100-w}) = \frac{c \cdot w}{5200} \times \log \tau(S_{\mathrm{PFSA,52wt\%}}) + \frac{c(100-w)}{1200} \times \log \tau(S_{\mathrm{PVP,12wt\%}}) \quad (3)$$

It is found that τ_M values of the PFSA/PVP/DMF solutions varying in compositions are approximately in accord with τ values calculated by the logarithmic mixing rule from their starting pure solutions. The τ_M values are higher than τ at the ratios of PFSA/PVP below 50/50. When it increases above 50/50, the experimental τ_M shows a slightly negative deviation with respect to τ. These are characteristic of the formation and strengthening of the polymer network by addition of PVP. With addition of PVP, the amide groups in PVP may interact with the $-SO_3^-$ groups of PFSA chains to destroy associating between ion groups, thus change the conformations of PFSA chains in DMF [50, 51]. Therefore, in the PFSA/PVP/DMF solutions, the PVP–PVP entanglements are diminished by the dilution effect of PFSA solution. On the other hand, new entanglements between PFSA and long coiled PVP chains are formed. Such newly formed entanglements will suppress the electrostatic repulsion interactions between ion groups and hence improve the electrospinnabilities of concentrated PFSA solutions.

At low PFSA/PVP ratios, PFSA molecules distribute among PVP chains and the R_f–SO_3^- groups interact with PVP. The new-formed PFSA-PVP entanglements make up

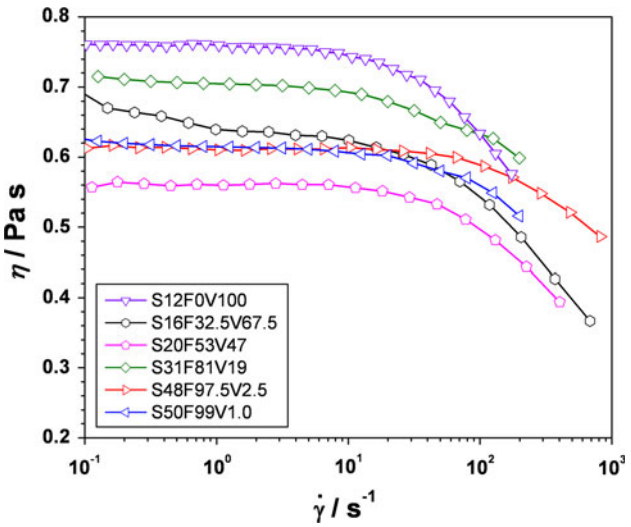

Fig. 6 Apparent viscosity η versus shear rate $\dot{\gamma}$ for PFSA/PVP solutions at 25 °C

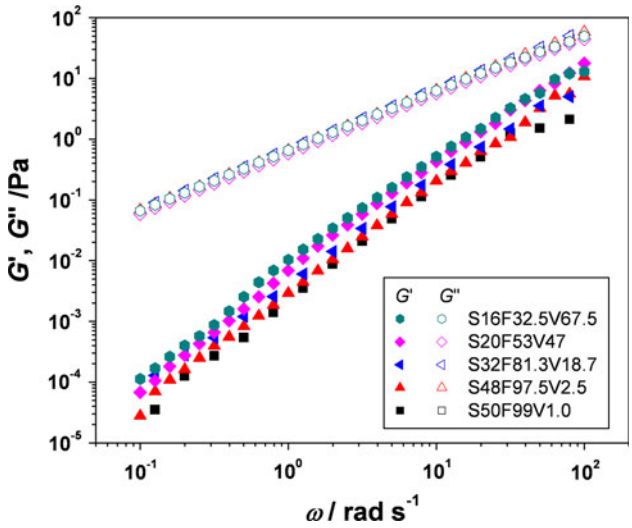

Fig. 7 Dynamic frequency sweeps of the PFSA/PVP/DMF at 25 °C. The *numbers* after the letters S, F, and V present the mass percentages of the total concentrations for the blend solutions, PFSA, and PVP in the blend polymers, respectively

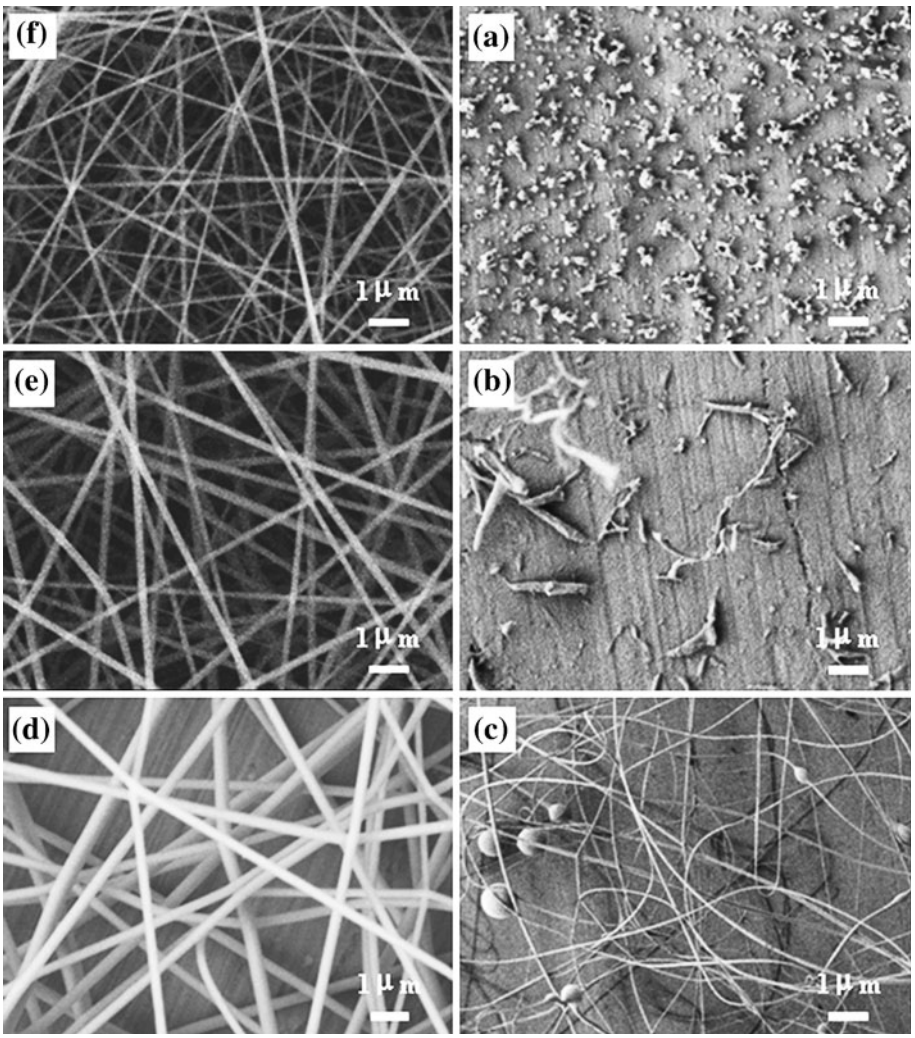

Fig. 8 SEM images of electrospun fibers of the PFSA/PVP blend solutions of **a** S52F100V0, **b** S50F99V1.0, **c** S48F97.5V2.5, **d** S32F81.3V18.7, **e** S20F53.0V47.0, and **f** S16F32.5V67.5

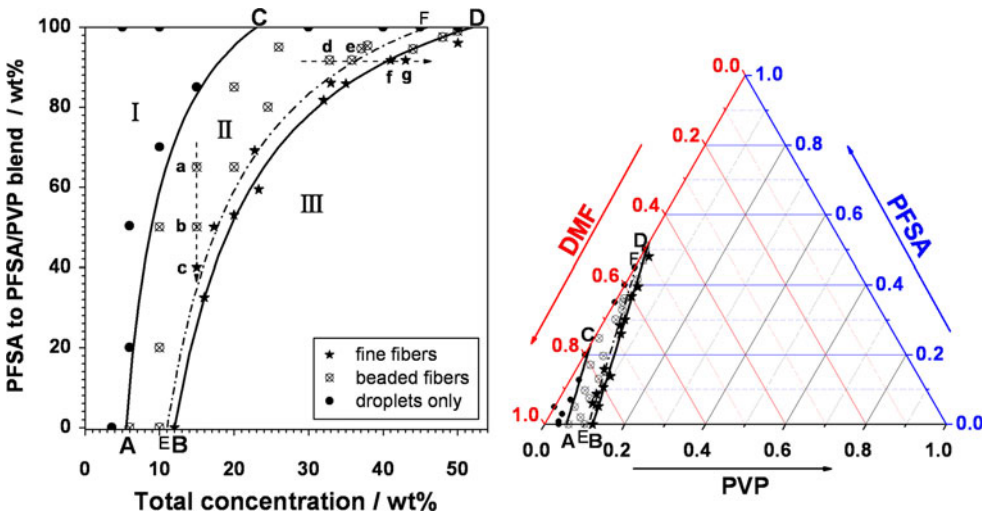

Fig. 9 Electrospun samples from PFSA/PVP/DMF solutions with different compositions. *I* droplets region, *II* beaded fibers region, *III* fine fibers region. The *lines* AC, BD, EF refer to the blend solutions prepared directly by mixing the two endpoint solutions of the *line* using principles of balance. (*a*) S15F65V35, (*b*) S15F50V50, (*c*) S15F40V60, (*d*) S32.8F92V8, (*e*) S35.8F92V8, (*f*) S41F92V8, and (*g*) S43F92V8

for or even exceed the lost of PVP–PVP entanglements. This would contribute a positive deviation from the theoretical curve with an improved electrospinnability. For a fixed total concentration of the mixed polymer solutions, increasing the weight percentage of PVP or increasing the total polymer concentration with a fixed PFSA/PVP ratio will improve the electrospinnability of the PFSA/PVP/DMF solution.

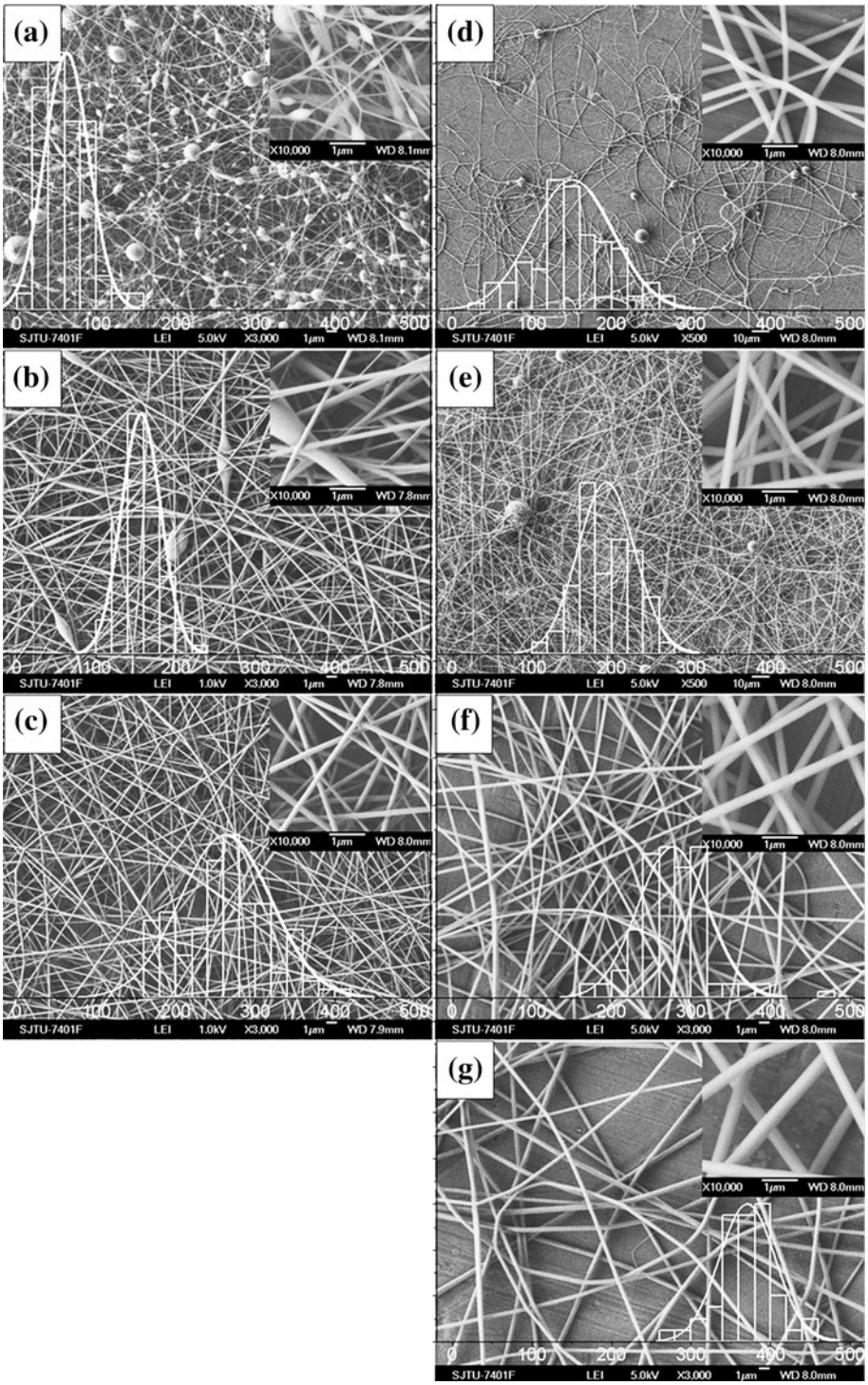

Fig. 10 SEM images and size distribution of electrospun fibers from PFSA/PVP blend solutions of **a** S15F65V35, **b** S15F50V50, **c** S15F40V60, **d** S32.8F92V8, **e** S35.8F92V8, **f** S41F92V8, and **g** S43F92V8

Electrospinning of PFSA/PVP blends

Electrospinning experiments were executed on the blend solutions with various total polymer concentrations and PFSA/PVP ratios. The feature of the nanofiber mats obtained from the PFSA/PVP/DMF ternary solutions with different compositions is presented in Fig. 9, and the typical SEM images of the electrospun fibers are shown in Fig. 10. For a fixed polymer concentration of 15 wt%(Fig. 9a–c), the morphologies of the electrospun samples changed from droplets, beaded fibers to continuous fibers with increasing PVP fraction in the total polymer from 35, 50 to 60 wt%, and the average diameters of the fibers increased from 62.7, 156.3 to 262.5 nm (Fig. 10a–c). For a fixed PFSA/PVP ratio of 92/8 (Fig. 9d–g), the morphologies of the electrospun samples were also improved

from droplets, beaded fibers to continuous fibers by increasing the total concentration from 32.8, 35.8, 41 to 43 wt%, with corresponding average diameters of the fibers increased from 150.85, 193.5, 276.9 to 370.7 nm (Fig. 10d–g). The diameters of the PFSA/PVP electrospun fibers are much smaller than that of the Nafion/PVP electrospun fibers (10 μm) from their blend solution in alcohol [52]. This may be ascribed to the higher boiling point of DMF than that of alcohol, thus giving the polymer chains longer time to be stretched before solidification.

It is interesting to find that the two adjacent regions of beaded fibers and fine fibers can be roughly divided by the thick solid line BD (Fig. 9), The solutions at this line can be readily prepared by mixing of $S_{PFSA,52wt\%}$ with the pure $S_{PVP,12wt\%}$ solution using principles of balance and leverage. These mixed solutions can be electrospun into fine nanofibers. Moreover, the mixed solutions at line EF can readily form fine fibers, while the two endpoint solutions of $S_{PVP,11wt\%}$ and $S_{PFSA,46wt\%}$ can not. This observation indicates that PVP seems to change the three-dimensional arrangement of PFSA chains in solution and further to improve the fiber formation capability, which agrees well with the rheological results.

Conclusions

The PFSA/PVP composite nanofibers with different composition ratios were prepared by electrospinning use DMF as solvent. The pure PVP/DMF forms bead-free fibers at ~12 wt% (about 2.18 C_e), following the "C_e-regulation" well, while the pure PFSA/DMF solutions with suitable surface tension fail to be electrospun even at high concentrations. Addition of PVP to PFSA/DMF solutions could effectively improve their electrospinnabilities. Bead-free fibers are successfully electrospun with suitable PFSA/PVP ratio. The mechanical relaxation time τ_M is a sensitive indicator for electrospinnabilities of PFSA/PVP/DMF solutions. And the τ_M values of the PFSA/PVP/DMF solutions are approximately in accord with those calculated by the logarithmic mixing rule from their starting pure solutions.

Acknowledgements The study was supported by the Ministry of Science and Technology 863 Hi-Technology Research and Development Program of China (2008AA11A106) and the Shanghai Leading Academic Discipline Project (No. B202).

References

1. Kim K, Yua M, Zong X, Chiuc J, Fang D, Seod YS, Hsiaoa BS, Chua B, Hadjiargyrou M (2003) Biomaterials 24:4977
2. Luong-Van E, Grødahl L, Chua KN, Leong KW, Nurcombe V, Cool SM (2006) Biomaterials 27:2042
3. Han D, Steckl AJ (2009) Langmuir 25:9454
4. Chen YB, Kim H (2009) Appl Surf Sci 255:7073
5. Wang S, Zhang Y, Yin G, Wang H, Dong Z (2009) J Appl Polym Sci 113:2675
6. Chen ZG, Wei B, Mo XM, Cui FZ (2009) J Polym Sci B 47:1949
7. Sill TJ, von Recum HA (2008) Biomaterials 29:1989
8. Ma H, Yoon K, Rong L, Mao Y, Mo Z, Fang D, Hollander Z, Gaiteri J, Hsiao BS, Chu B (2010) J Mater Chem 20:4692
9. Haider S, Park SY (2009) J Membr Sci 328:90
10. Picciani PHS, Medeiros ES, Pan Z, Orts WJ, Mattoso LHC, Soares BG (2009) J Appl Polym Sci 112:744
11. Roso M, Sundarrajan S, Pliszka D, Ramakrishna S, Modesti M (2008) Nanotechnology 19:285707
12. He J, Qin Y, Cui S, Gao Y, Wang S (2011) J Mater Sci 46:2938. doi:10.1007/s10853-010-5169-x
13. Virji S, Huang JX, Kaner RB, Weiller BH (2004) Nano Lett 4:491
14. Banerjee S, Curtin DE (2004) J Fluorine Chem 125:1211
15. Heitner-Wirguin C (1996) J Membr Sci 120:1
16. Nasef MM, Yahaya AH (2009) Desalination 249:677
17. Chiou JS, Paul DR (1988) Ind Eng Chem Res 27:2161
18. Matsuda M, Sekikawa T, Onodera K, Asama T, Chikama K, Inoue M, Kasai S (2003) Surg Endosc 17:1144
19. Liang HY, Qiu XP, Zhang SC, Zhu WT, Chen LQ (2004) J Appl Electrochem 34:1211
20. Hwang E, Levitsky IA, Euler WB (2010) J Appl Polym Sci 116:2425
21. Dai Z, Mohwald H (2002) Chem Eur J 8:4751
22. Harmer MA, Sun Q (2001) Appl Catal A 221:45
23. Vankelecom IFJ (2002) Chem Rev 102:3779
24. Laforgue A, Robitaille L, Mokrini A, Ajji A (2007) Macromol Mater Eng 292:1229
25. Nah C, Lee YS, Cho BH, Yu HC, Akle B, Leo DJ (2008) Compos Sci Technol 68:2960
26. Chen H, Snyder JD, Elabd YA (2008) Macromolecules 41:128
27. Veleirinho B, Rei MF, Lopes-Da-Silva JA (2008) J Polym Sci B 46:460
28. Patra SN, Easteal AJ, Bhattacharyya D (2009) J Mater Sci 44:647. doi:10.1007/s10853-008-3050-y
29. Shi Q, Vitchuli N, Nowak J, Lin Z, Guo B, McCord M, Bourham M, Zhang X (2011) J Polym Sci B 49:115
30. Talwar S, Hinestroza J, Pourdeyhimi B, Khan SA (2008) Macromolecules 41:4275
31. Peng Z, Yoshida Y, Sukigara S (2010) J Polym Sci B 48:1
32. Lee SJ, Yu TL, Lin HL, Liu WH, Lai CL (2004) Polymer 45:2853
33. Cirkel PA, Okada T, Kinugasa S (1998) Macromolecules 32:531
34. Johnson I, Kalidoss M, Srinivasamoorthy R (2002) J Chem Eng Data 47:1388
35. Li L, Hsieh Y-L (2005) Polymer 46:5133
36. Drew C, Wang X, Samuelson LA, Kumar J (2006) Electrostatic assembly of polyelectrolytes on electrospun fibers, vol 918. Polymeric Nanofibers. American Chemical Society, Washington, DC. doi:10.1021/bk-2006-0918.ch010
37. McKee MG, Wilkes GL, Colby RH, Long TE (2004) Macromolecules 37:1760
38. McKee MG, Hunley MT, Layman JM, Long TE (2006) Macromolecules 39:575
39. Subramanian C, Weiss RA, Shaw MT (2010) Polymer 51:1983
40. Ferry JD (1980) In: Ferry JD (ed) Viscoelastic properties of polymers, 3rd edn. Wiley, New York, p 57
41. Takahashi Y, Umeda M, Noda I (1988) Macromolecules 21:2257
42. Szajdzinska-Pietek E, Schlick S (1994) Langmuir 10:2188

43. Dobrynin AV, Colby RH, Rubinstein M (1995) Macromolecules 28:1859
44. Ma CH, Yu TL, Lin HL, Huang YT, Chen YL, Jeng US, Lai YH, Sun YS (2009) Polymer 50:1764
45. Barrat JL, Joanny F (1995) Adv Chem Phys 94:1
46. Li T, Zhong G, Fu R, Yang Y (2010) J Membr Sci 354:189
47. Wu HL, Ma CCM, Kuan HC, Wang CH, Chen CY, Chiang CL (2006) J Polym Sci B 44:565
48. Varesano A, Aluigi A, Vineis C, Tonin C (2008) J Polym Sci B 46:1193
49. Macaúbas PHP, Demarquette NR (2001) Polymer 42:2543
50. Hild A, Séquaris J, Narres H, Schwuger M (1998) Progr Colloid Polym Sci 111:174
51. Klech CM, Cato AE, Suttle AB (1991) Colloid Polym Sci 269:643
52. Bajon R, Balaji S, Guo SM (2009) J Fuel Cell Sci Technol 6:0310011